

Atomically localized plasmon enhancement in monolayer graphene

Wu Zhou^{1,2*}, Jaekwang Lee^{1,2}, Jagjit Nanda², Sokrates T. Pantelides^{1,2}, Stephen J. Pennycook^{1,2} and Juan-Carlos Idrobo^{1,2*}

Plasmons in graphene^{1–4} can be tuned by using electrostatic gating or chemical doping^{5–7}, and the ability to confine plasmons in very small regions could have applications in optoelectronics^{8,9}, plasmonics^{10,11} and transformation optics¹². However, little is known about how atomic-scale defects influence the plasmonic properties of graphene. Moreover, the smallest localized plasmon resonance observed in any material to date has been limited to around 10 nm (refs 13–15). Here, we show that surface plasmon resonances in graphene can be enhanced locally at the atomic scale. Using electron energy-loss spectrum imaging in an aberration-corrected scanning transmission electron microscope, we find that a single point defect can act as an atomic antenna in the petahertz (10^{15} Hz) frequency range, leading to surface plasmon resonances at the subnanometre scale.

A long-term goal of electronics has been to make devices smaller, faster, lighter and cheaper. However, after several decades of continuous development, the size of transistors, the building blocks for modern electronics, is approaching a limit imposed by nature and cost. Moreover, with the shrinking size and increasing packing density, leakage current and heat dissipation have become major problems¹⁶. One promising solution is to integrate optics with nanoelectronic devices and use light to transmit data^{17,18}. The major drawback, however, is the orders of magnitude mismatch between the micrometre-sized optical waveguides and the nanometre-sized active electronic components. Controlling and manipulating light at scales substantially smaller than its wavelength, with a view to achieving a seamless integration of optoelectronic devices, could result in new basic building blocks for future computers^{17,18} and represents the emerging field known as nanoplasmonics^{13,19–21}.

Surface plasmons, which are collective oscillations of electron density at the interface between two materials^{13,19–21}, hold promise in bridging the gap in scale. So far, research in nanoplasmonics has almost exclusively focused on the surface plasmons of metallic nanostructures on dielectric substrates^{13–15,19,21}, which unfold on a characteristic scale of 2–20 nm (ref. 21), with a reported record of $\lambda/40$ (ref. 14), where λ is the wavelength of the related plasmon excitation. However, the use of three-dimensional objects and the so-called non-locality length²¹ limit the length scale for any noble-metal plasmonic devices to the nanometre scale. This raises two questions: how can we go smaller, and how small can we go?

In this Letter, we report that the surface plasmon resonance in graphene can be locally enhanced at the subnanometre scale by the presence of single point defects, representing a length scale smaller than $\lambda/200$. Our results suggest that doped monolayer graphene could be used in the development of atomic-scale nanoplasmonics and quantum plasmonic devices. We studied the surface plasmon resonances of graphene using electron energy-loss (EEL)

spectrum imaging²² in an aberration-corrected scanning transmission electron microscope (STEM) (see Methods). The experiments were performed at an accelerating voltage of 60 kV, which is below the knock-on damage threshold of graphene. Annular dark-field (ADF) imaging was used to obtain structural and chemical information²³, atom by atom, around point defects in the graphene.

Figure 1a presents an ADF image of graphene, with a point defect located close to the centre of the image, and the edge of a second layer (lower right corner). A magnified view of the area enclosed by the white square in Fig. 1a is provided in Fig. 1b together with an overlaid structural model of the point defect derived from the experimental ADF and EEL spectrum imaging, first-principles calculations and image simulations (Supplementary Figs S2 and S3). The point defect consists of two adjoining fivefold rings formed by the exchange of two carbon atoms for one silicon atom, and a substitutional nitrogen atom bonded directly with the silicon atom (Fig. 1c–e).

The optical response of monolayer graphene is dominated by two main absorption peaks at ~ 4.5 eV and ~ 15 eV, which are commonly referred to as the π and $\pi + \sigma$ surface plasmons²⁴, respectively (Supplementary Fig. S10). To explore how the surface plasmons (π and $\pi + \sigma$) in graphene are affected by the presence of the point defect, we performed EELS line scans and spectrum imaging at the point-defect complex. Plasmon maps or intensity line profiles were obtained by integrating the EEL spectra at different energy ranges without any data processing (background subtraction or filtering of any sort).

Figure 2 shows an ADF signal and EELS line scan, simultaneously collected over a larger spatial range from the point defect shown in Fig. 1b. The presence of the double-layer graphene close to this point defect induced a continuously decaying background in the integrated $\pi + \sigma$ plasmon intensity line profile. This continuous decay, as a function of distance from the double-layer graphene region, can be modelled with an exponential decay function as shown in Fig. 2b. Importantly, the $\pi + \sigma$ plasmon intensity (integrated over an energy range of 11–18 eV) was found to be locally enhanced by the presence of the single point defect, with the maximum measured intensity centred at the silicon atom (Fig. 2b). The difference between the experimental integrated plasmon intensity and the exponential fit shows the spatial range over which the $\pi + \sigma$ plasmon is enhanced by the point defect. The full-width at half-maximum (FWHM) of this range is 0.43 ± 0.05 nm.

EEL spectrum images further provide the two-dimensional spatial distribution of this localized plasmon enhancement effect at the defect site. As shown in Supplementary Fig. S4, the local enhancement of the $\pi + \sigma$ plasmon can be observed directly from the raw

¹Department of Physics and Astronomy, Vanderbilt University, Nashville, Tennessee 37235, USA, ²Materials Science and Technology Division, Oak Ridge National Laboratory, Oak Ridge, Tennessee 37831, USA. *e-mail: wu.zhou@vanderbilt.edu; idrobojc@ornl.gov.

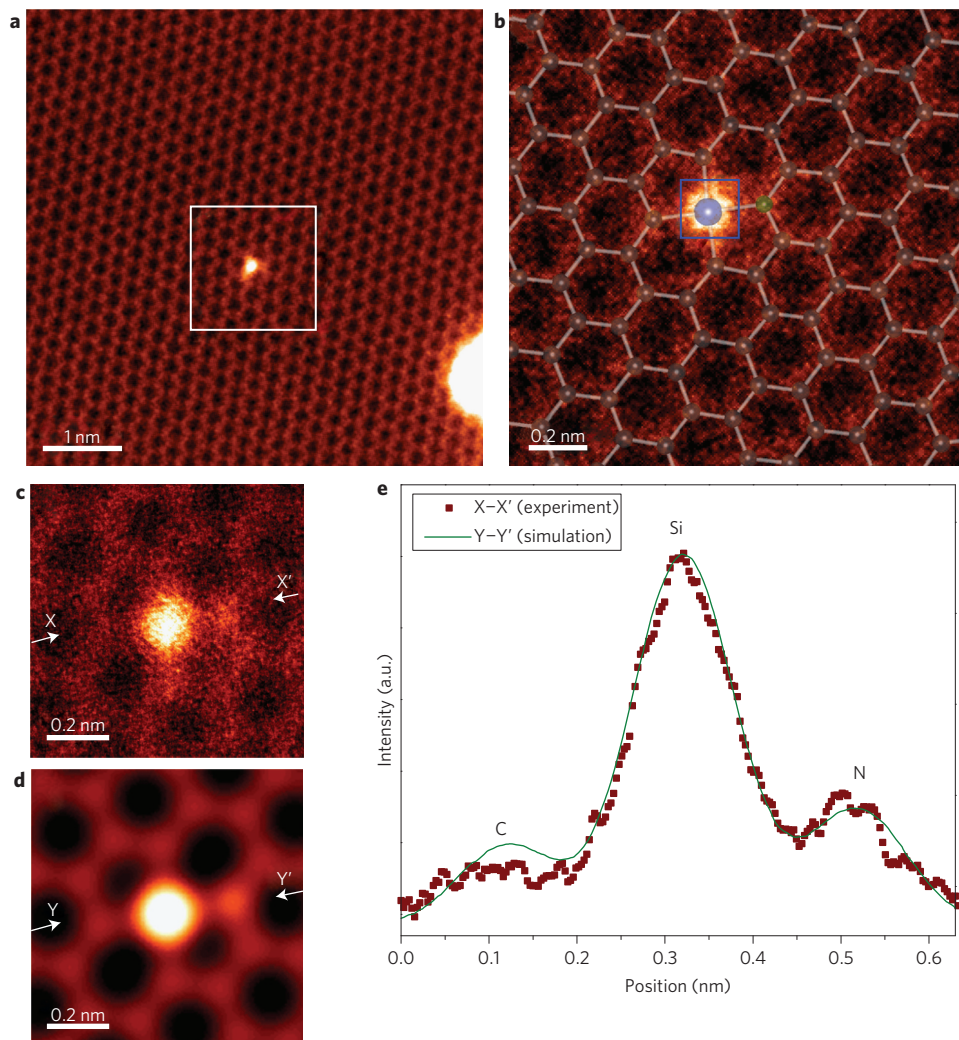


Figure 1 | Atomic structure of a point defect complex in monolayer graphene. **a**, ADF image showing the presence of the dopant atoms (and a fraction of the multilayer graphene at the lower right of the image). **b**, ADF survey image and overlaid structural model (carbon, silicon and nitrogen atoms shown in grey, blue and green, respectively) showing the specific area that was used for spectrum imaging. **c,d**, Magnified views of the substitutional silicon and nitrogen atoms: experimental ADF image taken after spectrum imaging (**c**) and simulated ADF image based on the relaxed structural model shown in **b** (**d**). **e**, Intensity profiles along X-X' and Y-Y' in the experimental (**c**) and simulated (**d**) images, respectively. Experimental images have been low-pass filtered.

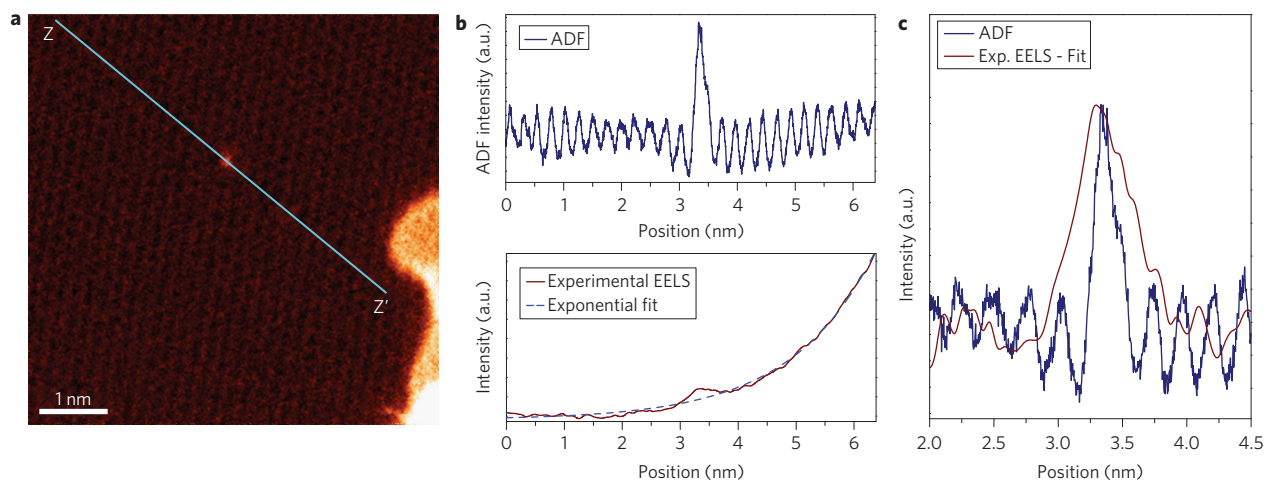


Figure 2 | STEM-EELS line scan across a point defect in monolayer graphene. **a**, Low-pass filtered ADF survey image. **b**, Simultaneously collected ADF and integrated EELS signals from 11–18 eV (raw data) as a function of probe position along the line (Z-Z') indicated in **a**. **c**, Comparison of the FWHM between the ADF signal and the enhanced plasmon intensity from the substitutional silicon atom.

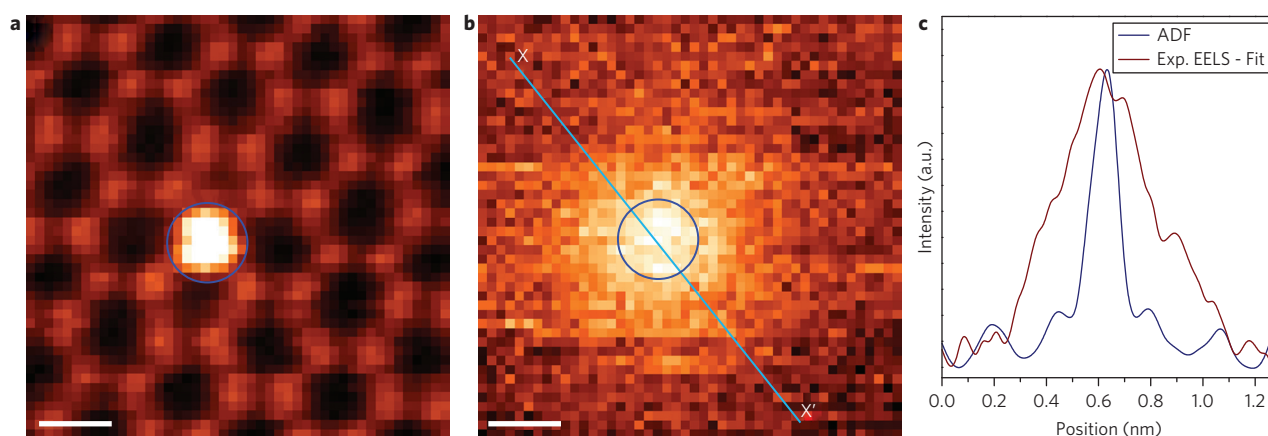


Figure 3 | Plasmon map of monolayer graphene with a single substitutional silicon atom. **a**, Simultaneous ADF image showing the atomic structure of the point defect. The blue circle indicates the position of the silicon atom. Subpixel scanning was not applied. **b**, Plasmon map (11–18 eV, raw data) showing localized enhancement of the $\pi + \sigma$ plasmon at the silicon atom. **c**, Comparison of the FWHM between the ADF signal and the enhanced plasmon intensity from the substitutional silicon atom. Line intensity profiles were taken along line X–X' in **b**. FWHM of the spatial range over which the $\pi + \sigma$ plasmon is enhanced is 0.41 ± 0.03 nm. Scale bars, 0.2 nm.

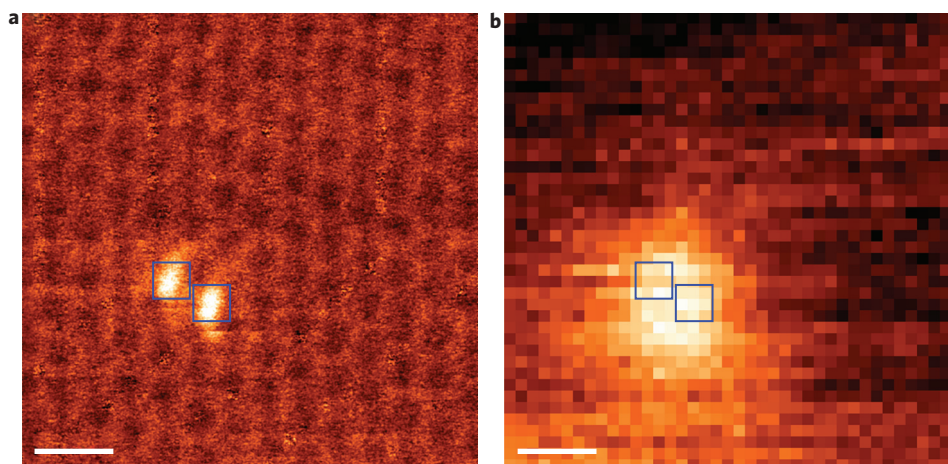


Figure 4 | Plasmon map of monolayer graphene with two adjacent substitutional silicon atoms far away from multilayer regions. **a**, ADF image collected simultaneously during spectrum imaging showing the presence of two substitutional silicon atoms. Subpixel scanning was applied during data acquisition. **b**, Plasmon map obtained from the raw data for the energy range 11–18 eV. Localized enhancement of the $\pi + \sigma$ plasmon was observed over both silicon atoms, as highlighted by the two blue squares. Note some vertical elongation is present owing to specimen drift and the presence of the multilayer region 4.7 nm below the defect sites (Supplementary Fig. S15), which superimposes a decaying background in the plasmon map. Scale bars, 0.5 nm.

data (Supplementary Fig. S4a) and from the filtered plasmon maps using principal component analysis (Supplementary Fig. S4b,c), which removes the decaying background induced by the nearby double-layered graphene. The enhanced plasmon intensity shows a maximum at the silicon atom with an extended tail at the nitrogen atom (Supplementary Fig. S4).

We also obtained an EEL spectrum image at a different point defect located far away from any multilayer graphene (Fig. 3). This point defect consists of two adjoining fivefold rings formed by the exchange of two carbon atoms for one silicon atom (Fig. 3a and Supplementary Fig. S9). The $\pi + \sigma$ plasmon map from the raw data (Fig. 3b) clearly shows a symmetric enhancement localized at the silicon atom, with the FWHM of the spatial range similar to that obtained from Fig. 2. In comparison, the $\pi + \sigma$ plasmon in defect-free graphene was found to be quite delocalized in space without any local enhancement (Supplementary Fig. S14d).

It should be mentioned that the two specific point-defect complexes shown in Figs 1 to 3 were highly stable under the electron beam, and no structural modification was observed during the acquisition of multiple EEL spectrum imaging data sets. The high

structural stability was further confirmed by density functional theory calculations (see Supplementary Information).

The localized enhancement of the surface plasmon at the point defects indicates that the substitutional silicon atoms act like atomic antennas or plasmonic enhancers in the petahertz range (11 eV is equivalent to a wavelength of ~ 113 nm or a frequency on the order of 1×10^{15} Hz). By atomically engineering or self-assembling substitutional silicon atoms in graphene, for example along grain boundaries or into linear arrays at interfaces, high-frequency signals could be transmitted along these atomically confined paths, and atomic-scale plasmonic/optoelectronic devices would be made possible. As a proof-of-concept testing, we mapped out the surface plasmon resonance of graphene with two adjacent substitutional silicon atoms (Fig. 4). As shown in Fig. 4b, the $\pi + \sigma$ surface plasmon intensity of graphene was locally enhanced over both silicon atoms, clearly coupling them, implying that a line of silicon atoms could act as a plasmonic waveguide. Moreover, with a rough estimation (Supplementary Fig. S16), the signal-to-background ratio is amplified by a factor of 2.3 compared with the case of a single silicon atom (Fig. 2). If more substitutional

silicon atoms were to line up in the graphene layer, we expect that this signal would be further amplified.

Similar to the $\pi + \sigma$ surface plasmon, localized enhancement was also observed for the π surface plasmon at the defect sites (Supplementary Figs S8b, S12d). However, it is difficult to quantify the enhancement on the π plasmon because of the proximity to the tail of the zero loss peak (ZLP), as shown in Supplementary Figs S11 and S12. A quantitative measurement of the localized plasmon enhancement effect, especially for the π plasmon, would require recording the ZLP and removal of the ZLP tail from the plasmon spectra, an experiment that is not yet possible with our current EEL spectrometer.

Several effects could be responsible for the atomically localized plasmon enhancement we observed experimentally. Excitonic effects, that is, electron–hole interactions, have been proposed to play an important role in the optical response of graphene^{25,26}. It was recently suggested, using first-principles calculations, that a resonant weakly bound exciton, spatially localized, can exist in graphene with optical excitations at 4.5 eV and 12.54 eV (refs 25,26). Additionally, theoretical calculations based on a non-local quantum-mechanical model also suggest that impurities in graphene could induce localized plasmonic modes²⁷. It has also been reported that dopants can modify the band structure of graphene near the Dirac point by coupling between electrons and plasmons²⁸. We speculate that the point defects, with impurities, might behave like a spatially localized bound exciton that can be used to control the optical response of graphene at the subnanometre scale. Moreover, the much stronger field confinement and enhanced light–matter interactions for graphene plasmons²⁹ may also help localize the plasmon enhancement at the defect sites. Further theoretical and experimental efforts are needed to fully understand the mechanism of this atomically localized plasmon enhancement effect.

The atomically localized surface plasmon resonances observed at point defects in monolayer graphene represent a length scale smaller than $\lambda/200$, and suggest that the physical limit for the size of plasmonic and optoelectronic devices can be down to the single atom level. Our observations also open up exciting possibilities for designing atomic-scale optoelectronic and plasmonic devices by assembling single atoms on monolayer graphene sheets. By using different dopant atoms, such as boron, nitrogen, iron, silver or gold, it may also be possible to tune the enhancement of the plasmon resonance to different energy (frequency) ranges²⁷. From a fundamental perspective, it would also be interesting to explore the scattering and absorption of surface plasmons in graphene when the substitutional atoms are assembled into different geometrical shapes, such as quantum corrals³⁰. Aberration-corrected STEM, as demonstrated in this study, provides an ideal means to characterize such devices and explore the optical response of materials at the single atom level.

Methods

Sample preparation. The graphene sample for STEM analysis was obtained from Graphene-Supermarket. The graphene material was grown on a nickel film on a silicon wafer using a chemical vapour deposition (CVD) method. The graphene layers were then extracted from the nickel film via chemical etching using concentrated nitric acid, and deposited onto a 2,000-mesh copper grid. The sample contained both monolayer and multilayer graphene.

STEM-EEL spectrum imaging experiments. The experiments were performed with a Nion UltraSTEM, equipped with a cold field-emission electron source and a corrector of third- and fifth-order aberrations, operating with a probe current of ~ 110 pA at an accelerating voltage of 60 kV. EEL spectra were collected using a Gatan Enigma spectrometer, with an energy resolution of 1 eV for 0.5 eV per channel dispersion, 0.6 eV for 0.3 eV per channel dispersion and 0.4 eV for 0.05 eV per channel dispersion. The convergence semi-angle for the incident probe was 31 mrad, with an EELS collection semi-angle of 48 mrad. Different energy dispersion and offset settings were used to collect the data shown in this Letter. Long dwell times, 0.05 s per pixel and 0.1 s per pixel, were adopted to increase the signal-to-noise ratio in the spectrum images. As limited by the dynamic range of the

charge-coupled device camera in our EEL spectrometer, the extremely intense ZLP could not be recorded into the spectrum image under the long dwell-time settings. The pixel size for spectrum imaging ranged from 0.2 Å to ~ 1 Å. ADF images were collected for a half-angle range of ~ 86 –200 mrad.

Image simulation, first-principles calculations and data processing. STEM-ADF image simulation was performed using the QSTEM simulation package with the atomic structural model of graphene defect shown in Fig. 1b, which was derived from experimental STEM-ADF imaging and EELS analysis and relaxed using first-principles methods. The first-principles calculations and the principal component analysis of the EEL spectrum imaging are described in more detail in the Supplementary Information.

Received 14 June 2011; accepted 20 December 2011;
published online 29 January 2012

References

- Geim, A. K. Graphene: status and prospects. *Science* **324**, 1530–1534 (2009).
- Abergel, D. S. L., Apalkov, V., Berashevich, J., Ziegler, K. & Chakraborty, T. Properties of graphene: a theoretical perspective. *Adv. Phys.* **59**, 261–482 (2010).
- Novoselov, K. S. *et al.* Electric field effect in atomically thin carbon films. *Science* **306**, 666–669 (2004).
- Berger, C. *et al.* Ultrathin epitaxial graphite: 2D electron gas properties and a route toward graphene-based nanoelectronics. *J. Phys. Chem. B* **108**, 19912–19916 (2004).
- Mak, K. F. *et al.* Measurement of the optical conductivity of graphene. *Phys. Rev. Lett.* **101**, 196405 (2008).
- Chen, C.-F. *et al.* Controlling inelastic light scattering quantum pathways in graphene. *Nature* **471**, 617–620 (2011).
- Wang, F. *et al.* Gate-variable optical transitions in graphene. *Science* **320**, 206–209 (2008).
- Liu, M. *et al.* A graphene-based broadband optical modulator. *Nature* **474**, 64–67 (2011).
- Bonaccorso, F., Sun, Z., Hasan, T. & Ferrari, A. C. Graphene photonics and optoelectronics. *Nature Photon.* **4**, 611–622 (2010).
- Jablan, M., Buljan, H. & Soljagic, M. Plasmonics in graphene at infrared frequencies. *Phys. Rev. B* **80**, 245435 (2009).
- Mishchenko, E. G., Shytov, A. V. & Silvestrov, P. G. Guided plasmons in graphene p–n junctions. *Phys. Rev. Lett.* **104**, 156806 (2010).
- Vakil, A. & Engheta, N. Transformation optics using graphene. *Science* **332**, 1291–1294 (2011).
- Maier, S. A. & Atwater, H. A. Plasmonics: localization and guiding of electromagnetic energy in metal/dielectric structures. *J. Appl. Phys.* **98**, 011101 (2005).
- Nelayah, J. *et al.* Mapping surface plasmons on a single metallic nanoparticle. *Nature Phys.* **3**, 348–353 (2007).
- Bosman, M., Keast, V. J., Watanabe, M., Maarouf, A. I. & Cortie, M. B. Mapping surface plasmons at the nanometre scale with an electron beam. *Nanotechnology* **18**, 165505 (2007).
- Theis, T. N. & Solomon, P. M. It's time to reinvent the transistor! *Science* **327**, 1600–1601 (2010).
- McAulay, A. D. *Optical Computer Architectures: The Application of Optical Concepts to Next Generation Computers* (Wiley, 1991).
- Caulfield, H. J. & Dolev, S. Why future supercomputing requires optics. *Nature Photon.* **4**, 261–263 (2010).
- Barnes, W. L., Dereux, A. & Ebbesen, T. W. Surface plasmon subwavelength optics. *Nature* **424**, 824–830 (2003).
- Ozbay, E. Plasmonics: merging photonics and electronics at nanoscale dimensions. *Science* **311**, 189–193 (2006).
- Stockman, M. I. Nanoplasmonics: the physics behind the applications. *Phys. Today* **64**, 39–44 (2011).
- Hunt, J. A. & Williams, D. B. Electron energy-loss spectrum-imaging. *Ultramicroscopy* **38**, 47–73 (1991).
- Krivanek, O. L. *et al.* Atom-by-atom structural and chemical analysis by annular dark-field electron microscopy. *Nature* **464**, 571–574 (2010).
- Gass, M. H. *et al.* Free-standing graphene at atomic resolution. *Nature Nanotech.* **3**, 676–681 (2008).
- Yang, L., Deslippe, J., Park, C.-H., Cohen, M. L. & Louie, S. G. Excitonic effects on the optical response of graphene and bilayer graphene. *Phys. Rev. Lett.* **103**, 186802 (2009).
- Yang, L. Excitons in intrinsic and bilayer graphene. *Phys. Rev. B* **83**, 085405 (2011).
- Muniz, R. A., Dahal, H. P., Balatsky, A. V. & Haas, S. Impurity-assisted nanoscale localization of plasmonic excitations in graphene. *Phys. Rev. B* **82**, 081411 (2010).
- Bostwick, A. *et al.* Observation of plasmarons in quasi-freestanding doped graphene. *Science* **328**, 999–1002 (2010).
- Koppens, F. H. L., Chang, D. E. & Javier Garcia de Abajo, F. Graphene plasmonics: a platform for strong light–matter interactions. *Nano Lett.* **11**, 3370–3377 (2011).

30. Crommie, M. F., Lutz, C. P. & Eigler, D. M. Confinement of electrons to quantum corrals on a metal surface. *Science* **262**, 218–220 (1993).

Acknowledgements

The authors thank B.S. Guiton, S.V. Kalinin, R.F. Klie, A.R. Lupini, and M.P. Oxley for helpful discussions and comments. This research was supported by the National Science Foundation (grant no. DMR-0938330; W.Z., J.-C.I.); Oak Ridge National Laboratory's (ORNL) SHaRE User Facility (J.C.I.), which is sponsored by the Office of Basic Energy Sciences, US Department of Energy (DOE); the Office of Basic Energy Sciences, Materials Sciences and Engineering Division, US DOE (S.J.P., J.L., S.T.P.), DOE grant DE-FG02-09ER46554 (S.T.P.); and by the McMinn Endowment (S.T.P.) at Vanderbilt University. This research used resources of the National Energy Research Scientific Computing Center, which is supported by the Office of Science of the US DOE (contract no. DE-AC02-05CH11231).

Author contributions

W.Z, J.N., S.J.P. and J.-C.I. conceived the experiments. W.Z. and J.-C.I. designed and carried out the experiments, performed the data analysis, and co-wrote the paper. W.Z. performed the image simulations. J.L., S.T.P. and J.-C.I. performed the first-principles calculations. J.N. provided the sample. S.J.P. initiated the aberration-corrected microscopy project at ORNL and provided advice regarding the manuscript. All authors discussed the results and commented on the manuscript.

Additional information

The authors declare no competing financial interests. Supplementary information accompanies this paper at www.nature.com/naturenanotechnology. Reprints and permission information is available online at <http://www.nature.com/reprints>. Correspondence and requests for materials should be addressed to W.Z. and J.-C.I.